THE ASTROPHYSICAL JOURNAL, 377:434–441, 1991 August 20

THE MOLECULAR STRUCTURE OF A STARBURST: ^{13}CO IN THE NUCLEUS OF MAFFEI 2

ROBERT L. HURT[1]
Department of Physics, UCLA
AND
JEAN L. TURNER[1]
Department of Astronomy, UCLA
Received 1990 August 1; accepted 1991 February 4

ABSTRACT

We present high-resolution ($\sim 6''$) maps of the ^{13}CO emission in the nucleus of the nearby spiral galaxy Maffei 2 made with the Owens Valley Millimeter Interferometer. The optically thin ^{13}CO emission, a tracer of H_2 gas density, indicates that the molecular cloud distribution in the nucleus of Maffei 2 is remarkably well-correlated with the starburst as traced by radio continuum emission. Evidently the molecular density distribution determines the spatial structure of this starburst. The observed range of ^{13}CO emission implies H_2 column densities of $N_{H_2} = 0.13\text{–}1.3 \times 10^{32}$ cm^{-2}, molecular surface densities of $\sigma_{H_2} = 200\text{–}2000\ M_\odot$ pc^{-2}, and visual extinctions of $A_V = 14\text{–}140$ mag on size scales of ~ 150 pc. The molecular material forms a barlike structure 40″ (1 kpc at an assumed distance of 5 Mpc) in extent, with a total H_2 mass of $M_{H_2} = 2.3 \times 10^8\ M_\odot$. Two dynamical components are evident in the ^{13}CO maps: a region within ~ 120 pc of the nucleus that appears to rotate rapidly as a solid body; then nearly Keplerian fall-off to a less-rapidly rotating region extending to a radius of ~ 500 pc. The most intense star formation activity appears in the inner solid body region of the rotation curve. Within the solid body region, gas accounts for $\sim 40\%$ of the estimated dynamical mass. The centroid of the molecular mass is offset by ~ 120 pc from the dynamical center of the galaxy. Since the dynamical time scale against winding by differential rotation is $\sim 10^6$ yr, some mechanism must contribute to the longevity of this nuclear bar structure, possibly spiral density waves.

Subject headings: galaxies: individual (Maffei 2) — galaxies: interstellar matter — galaxies: nuclei — stars: formation

1. INTRODUCTION

Starbursts are active star-forming regions with rates of massive star formation of $\gtrsim$ a few $M_\odot$ yr^{-1}, comparable to the total star formation rate of the entire Milky Way (Tinsley 1980), but confined to regions of a few hundred parsecs in extent (Rieke & Lebofsky 1978; Rieke et al. 1980; Becklin et al. 1980; Telesco & Harper 1980). In nearby galaxies, unusually active star-forming regions are often located near the nucleus (Israel 1980; Condon et al. 1982). What precipitates such intense star formation, and how is it fueled? Why is it often located in the nucleus and how is it related to the molecular gas distribution and kinematics there? High spatial resolution studies of molecular gas in the nuclei of nearby starbursts are important in addressing some of these questions.

Maffei 2 is an S(B)bc galaxy at a distance of ~ 5 Mpc (Spinrad et al. 1971, 1973). Maffei 2 is in the Galactic plane ($l = 136°$, $b = -0.°5$) with foreground visual extinction of $A_V \cong 5$ mag (Spinrad et al. 1971; Buta & McCall 1983). Strong infrared (Rieke & Lebofsky 1978; Rickard & Harvey 1983), Brackett line (Ho, Beck, & Turner 1990) and radio continuum emission (Seaquist, Pfund, & Bignell 1976; Turner & Ho 1990) indicate that the nucleus is the site of a moderately strong starburst of $L_{FIR} \sim 4 \times 10^9\ L_\odot$ (Rickard & Harvey 1983, 1984). Bright 6 cm continuum emission in the nucleus of Maffei 2 is over two orders of magnitude more intense than typical extended spiral disk emission (Ekers 1975) and is likely due to H II regions and young SNRs directly associated with the starburst (Turner & Ho 1991). This interpretation is supported by the presence of an intense 10 μm emission region (Ho et al. 1989; C. M. Telesco, private communication) that is spatially coincident with this bright radio continuum emission. H I studies indicate nonaxisymmetric distortions in the velocity field near the nucleus suggestive of bar-streaming motions (Shostak & Weliachew 1971; Bottinelli et al. 1971; Hurt, Turner, & Ho 1991). Observations of the ^{12}CO $J = 1\text{–}0$ (Rickard, Turner, & Palmer 1977) and $J = 2\text{–}1$ (Sargent et al. 1985) lines suggest that the molecular gas is strongly concentrated within the inner 750 pc with noncircular motions near the nucleus (Weilachew, Casoli, & Combes 1988). High-resolution ^{12}CO (1–0) maps from the Nobeyama Millimeter Array (Ishiguro et al. 1989) show a central molecular bar of $\sim 1'$ (1.5 kpc) in extent.

In this paper we present maps of Maffei 2 in the ^{13}CO $J = 1\text{–}0$ transition at 6″–7″ resolution made with the Owens Valley Millimeter Interferometer. Since ^{13}CO clouds have a lower optical depth than ^{12}CO clouds, we are able to trace the molecular density structure with greater fidelity than previous studies. Our maps indicate that the molecular clouds in the nucleus of Maffei 2 form a barlike structure that is remarkably well-correlated with the radio continuum emission from the starburst. We argue that this structure is likely to be due to a one-armed spiral density wave. Within this molecular material we see two kinematically distinct components: the center which is compact and rotating rapidly with a steep velocity gradient, and the extended bar which has a flattened rotation curve.

[1] Postal address: Department of Astronomy, UCLA, 405 Hilgard Avenue, Los Angeles, CA 90024

2. OBSERVATIONS AND RESULTS

Aperture synthesis maps of the nuclear region of Maffei 2 in the ^{13}CO $J = 1$–0 transition at 110.2014 GHz were made with the Owens Valley Radio Observatory (OVRO) Millimeter Interferometer between 1989 January and May. The interferometer is composed of three 10.4 m dishes with cryogenically cooled SIS receivers (Woody, Miller, & Wengler 1985). System temperatures referred to the top of the atmosphere ranged from 300 to 800 K (SSB) during the observations. The 32 channel 5 MHz filterbank gives a velocity resolution of 13.6 km s^{-1} with an overall bandwidth of 345 km s^{-1} and was centered at $V_{LSR} = -16.0$ km s^{-1} (corresponding to channel 16.5). The phase center of the maps is at $\alpha = 2^h38^m8^s.4$, $\delta = 59°23'30''$, the position of the 6 cm continuum peak (Turner & Ho 1991). The synthesized beamwidth (FWHM) is $6''.6 \times 6''.0$ (160 × 145 pc) at P.A. $-3°.7$. Table 1 summarizes observational parameters and results.

The phases were calibrated at 20 minute intervals using 0224+671. Absolute flux calibration was based on the fluxes of Mars and Uranus and is good to ~15%–20%. The naturally weighted maps were produced with the National Radio Astronomy Observatory (NRAO) AIPS software package. The rms noise in the channel maps is typically 10 mJy beam^{-1}, or 0.05 K. No continuum emission was detected in the 12 combined line-free channels above the 3 σ level. The signal-to-noise was improved in the integrated maps by blanking fluxes below the 1 σ level, then manually blanking the regions beyond the obvious line emission. The integrated intensity map was then corrected for the primary beam response of the OVRO dishes.

The ^{13}CO channel maps (Fig. 1) illustrate the overall molecular distribution and dynamics in the inner kpc of Maffei 2. Emission is detected in the inner 40″ (or 0.97 kpc) of the galaxy across a velocity range of 245 km s^{-1}. The range of detected antenna temperature of the emission is $T_A^* = 0.1$–0.9 K. Given that the ^{13}CO optical depths are $\tau_{^{13}CO} \sim 0.05$–0.2 (§ 3.1) we infer beam-averaged brightness temperatures of $T_b = 1$–5 K. By taking $T_{ex} = T_{dust} \sim 50$ K (Rickard & Harvey 1983), we estimate real filling factors of 2%–10% for the molecular gas. This adopted temperature is warmer than the 10–20 K typical of large Galactic disk molecular clouds (Scoville & Good 1989), but similar to those seen in the nuclear regions of M82 (Lo et al. 1987), IC 342 (Ho, Turner, & Martin 1987), and our own Galactic center (Morris et al. 1983). Negative sidelobes in the 18.0 km s^{-1} channel, and to a lesser extent in the −90.8, 4.4, 31.6, and 86.0 km s^{-1} channels, suggest the emission may have been undersampled at these velocities, indicating structures $\gtrsim 40''$ in extent. We detect a total integrated flux of 148 Jy km s^{-1}, representing ~65% of the single dish flux detected in this region with the arcminute beam of the NRAO 12 m Telescope (R. Martin, private communication). The missing flux may be accounted for by undersampling and absolute flux calibration errors.

TABLE 1

MAFFEI 2

Property	Value
Distance[a,b]	5 Mpc
Inclination[b]	66°
Position angle[b]	26°
Extent of ^{13}CO emission region	40″ × 12″(1.0 × 0.3 kpc)
^{13}CO Total flux	157 km s^{-1}
$V_{sys}(^{13}CO)$	-10 ± 5 km s^{-1}
Dynamical center	$\alpha = 2^h38^m8^s.25 \pm 0^s.15$
	$\delta = 59°23'27 \pm 2''$
^{13}CO Integrated intensity peak	$\alpha = 2^h38^m8^s.43 \pm 0^s.05$
	$\delta = 59°23'30 \pm 1''$
Total H_2 mass[c]	$2.3 \times 10^8 M_\odot$
H_2 Mass (inner 500 pc radius)[c]	$1.2 \times 10^8 M_\odot$
Total gas mass (including He)[c]	$3.1 \times 10^8 M_\odot$
Gas mass (inner 500 pc radius)[c]	$1.6 \times 10^8 M_\odot$
Dynamical mass (inner 500 pc radius)	$4 \pm 1 \times 10^8 M_\odot$

[a] Spinrad et al. 1973.

[b] Hurt, Turner, & Ho 1991.

[c] Gas masses are uncertain to at least a factor of 2 due to ^{13}CO fractionation effects (see text).

The overall kinematics of the nuclear region of Maffei 2 are characteristic of rotation. The channel maps indicate that there are two kinematically distinct components. The first is a spatially compact region of high-velocity gas within ~5″ (120 pc) of the dynamical center. This emission is most evident as a separate component in the −145.2 to −77.2 and 31.6 to 99.6 km s^{-1} channel maps, with an overall velocity width of ~245 km s^{-1}. A second, more spatially extended component appears over a more limited velocity range of ~160 km s^{-1} in the −104.4 to 58.8 km s^{-1} maps. For both components the variation in position of peak emission with velocity is consistent with rotation, with the highest rotational velocities near the nucleus. We treat the dynamics of the molecular gas in § 3.2.

The integrated ^{13}CO emission is shown in relation to the extended optical emission in Figure 2. The gray-scale image is a deep exposure red plus Hα image, showing the full extent of the galaxy. Spiral arm structure can be seen in the SW portion of the galaxy and to a lesser extent, in the NE. This spiral structure coincides with H I and 21 cm radio continuum emission (Hurt, Turner, & Ho 1990) which is consistent with a bar or spiral arms oriented in the same direction as the ^{13}CO emission (contours). A closeup of the nuclear region (Fig. 2*b*) shows that the region of greatest ^{13}CO intensity is centered at what appears to be a region of enhanced extinction through the nucleus. This is consistent with the high extinctions implied by the ^{13}CO intensities (§ 3.1).

The ^{13}CO integrated intensity map (Fig. 3*a*, contours) shows that the ^{13}CO emission in Maffei 2 forms a barlike structure of dimension 40″ × 12″, or 1 × 0.3 kpc, at an average position angle of 25°–30°. The 6″ beamwidth makes this value an upper limit to the true width of the bar, which could be as narrow as 150 pc. If the elongation of the emission were due to the inclination of a thin, circular disk of material, the observed eccentricity would require that it be inclined ~80° to our line of sight, correcting for beam broadening. H I studies indicate that the large-scale disk of Maffei 2 has an inclination of 66° at a position angle of 26° (Hurt, Turner, & Ho 1990). Thus the ^{13}CO emission would require a disk that is inclined with respect to the H I disk. A tilted disk has also been proposed for the gas in our own Galactic center (Burton & Liszt 1978; Liszt & Burton 1978; Sanders, Solomon, & Scoville 1984). However, to produce the elongated structure seen in Maffei 2, this model would require a fortuitous alignment of the axis of inclination of this nuclear disk with respect to our line-of-sight. A simpler description of the elongated morphology would be that of a nonaxisymmetric structure such as a bar, or very open spiral arms. The antisymmetric "S" shape of the emission region has been described as two nearly linear ridges of gas by Ishiguro et al. (1989). The position angle of the contours at the center of emission is ~10°–15° while the position angle for the outer contours is ~25°–30°, an overall difference of ~35° were the galaxy viewed face-on. This shift in positional angle is more

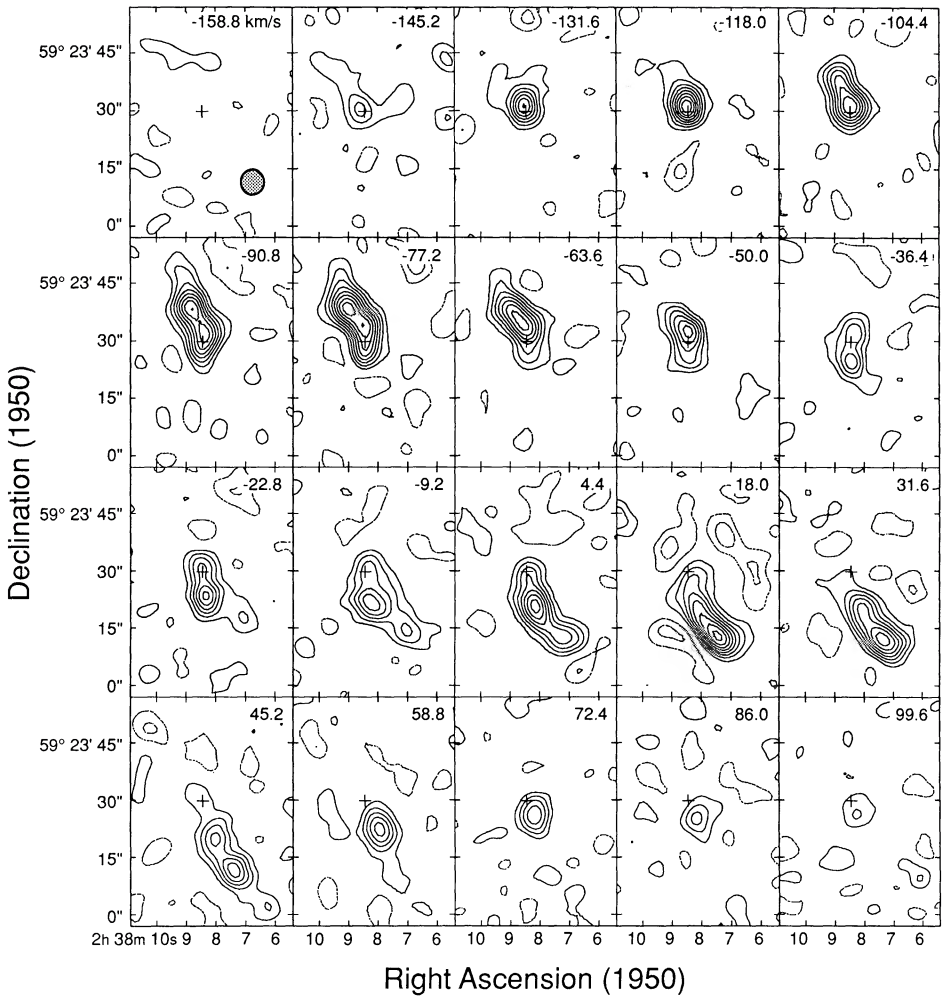

FIG. 1.—^{13}CO channel maps. Contours are plotted at 0.1 K (39 mJy beam^{-1}) intervals, corresponding to 2 σ levels. The beam size of 6.″6 × 6.″0 (P.A. −4°, indicated by gray oval, first channel) represents a linear resolution of 0.16 × 0.15 kpc at an assumed distance of 5 Mpc.

suggestive of spiral arms than a strictly linear bar. This structure is similar to molecular barlike features in other nearby face-on spirals like IC 342 (Lo et al. 1984) and NGC 6946 (Ball et al. 1985).

Underlying the ^{13}CO integrated intensity map contours in Figure 3*a* is a gray-scale image of radio continuum emission in Maffei 2 (Turner & Ho 1990). The 6 cm continuum emission is a mixture of thermal bremsstrahlung and nonthermal synchrotron emission from H II regions and SNR's in the central starburst. The correspondence between the molecular gas and the radio continuum emission is striking. A direct comparison made by convolving the continuum emission to the same beam size as the ^{13}CO emission shows that the ratio of 6 cm flux density to ^{13}CO intensity, $S_{6\text{cm}}/I_{^{13}\text{CO}}$, varies by a factor of only ~3 across the bulk of the molecular bar region, even into the region of weak continuum emission in the SW portion.

The intensity-weighted velocity moment map of Figure 3*b* shows that the rotation curve is steeply rising in the center, flattening out significantly in the bar. The isovelocity contours indicate that within the inner 10″ the rotation velocity of the gas increases sharply, consistent with uniform solid-body rotation in this region. The velocity becomes remarkably flat if somewhat irregular in the NE and SW extensions of the bar. This behavior is also clearly visible in the position-velocity diagram in Figure 4. These irregularities are due largely to the spatial asymmetry of the molecular distribution and, at the edges of the emission, low signal-to-noise. The large positive velocity peak to the SW of the nucleus, for example, is due to the high-velocity nuclear emission. A corresponding negative peak is not evident in the NE because the emission from the lower velocity bar material is stronger there.

We do not see the marked noncircular distortions in the velocity field observed in ^{12}CO (Ishiguro et al. 1989) and on larger scales in H I (Shostak & Weliachew 1971; Bottinelli et al. 1971; Hurt, Turner, & Ho 1990). Nonetheless, the isovelocity contours are inclined ~7° with respect to the minor axis of the galaxy as determined from H I (Hurt, Turner, & Ho 1990) which suggests that either there is a small warp near the center of the galaxy causing variations in position angle and inclination or there are small noncircular perturbations in the velocity field. If this distortion is interpreted as a uniform radial inflow across a disk that is otherwise exhibiting circular motion, which is consistent with the direction of the distortion, we estimate an inflow velocity on the order of 5 km s^{-1}. This interpretation assumes that the NW edge is the near side of the galaxy, implied by the overall sense of rotation and the direc-

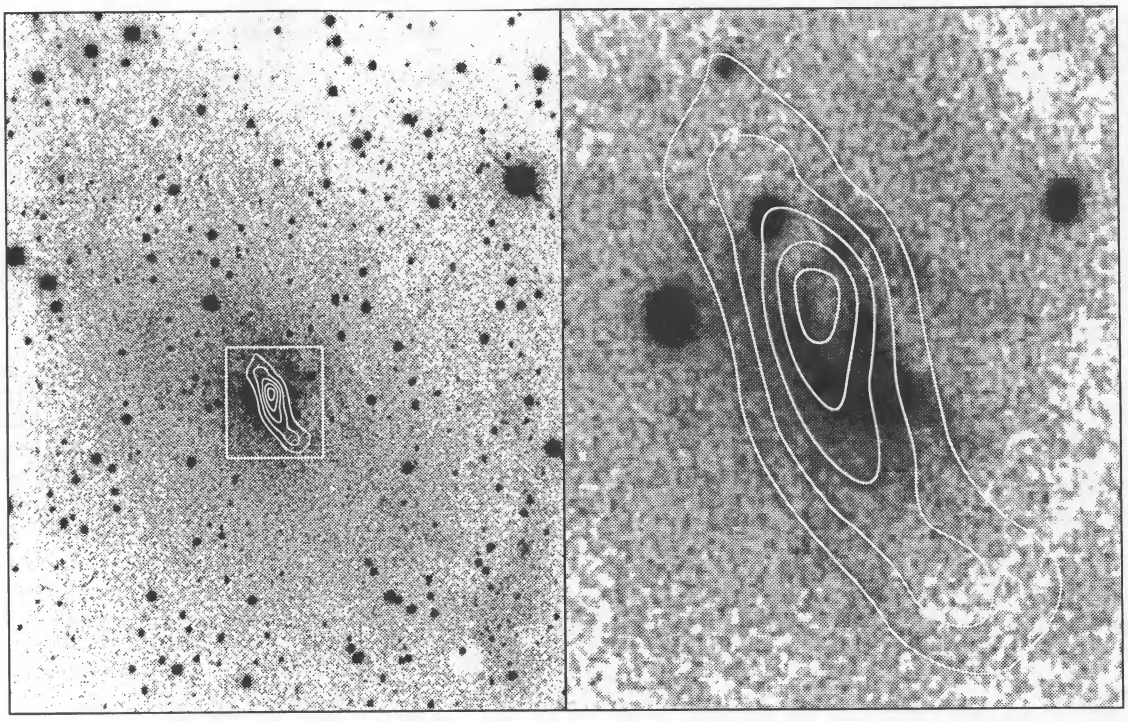

FIG. 2.—Integrated ^{13}CO/Optical emission comparison. The ^{13}CO integrated intensity map (contour) is overlaid on a deep-exposure red plate of Maffei 2 (Spinrad et al. 1973). Optical photometry is by D. Wills and P. McCarthy. Contour levels start at 13 K km s^{-1}, spaced at 26 K (10.2 Jy beam^{-1} km s^{-1}) intervals. *Left*: full galaxy, covering a field of view of $\sim 4' \times 5'$. Evident in the SW is a spiral arm structure that aligns with the ^{13}CO distribution. *Right*: detail of nucleus, covering a field of view of $\sim 35'' \times 45''$. The enhanced contrast in this region shows the alignment between the densest ^{13}CO emission and a "finger" of increased extinction in the nucleus, probably caused by dust clouds within the most intense star-forming region.

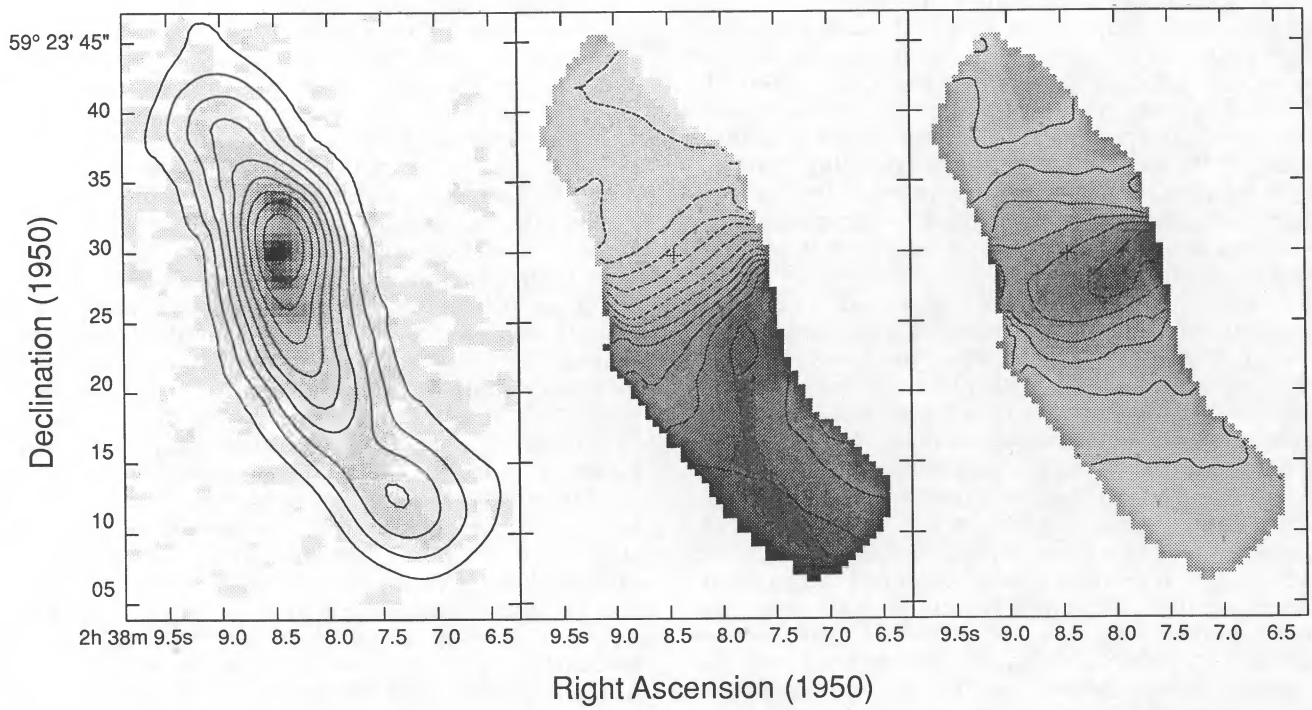

FIG. 3.—Intensity-weighted moment maps. *Left panel:* ^{13}CO integrated intensity map (contour) overlaid on a 1″ resolution 6 cm continuum map (Turner & Ho 1990; gray scale). Contour levels are at 13 K km s^{-1} (5 Jy beam^{-1} km s^{-1}) intervals. The gray-scale intensity range is 0.5–8 mJy beam^{-1}. *Middle panel:* intensity-weighted velocity moment map overlaid on a gray-scale representation of itself. Contour levels range from -70–50 km s^{-1} at 10 km s^{-1} intervals (negative contours are dashed, zero, and positive are solid). *Right panel*: Velocity second moment (dispersion) map, also overlaid on a gray-scale representation of itself. Contour levels range from Δv = 10–70 km s^{-1} ($V_{\rm FWHM}$ = 25–160 km s^{-1}) at 10 km s^{-1} intervals.

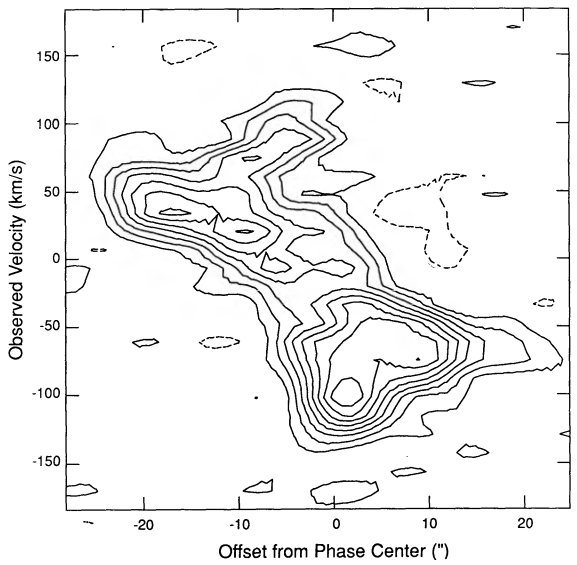

FIG. 4.—Position-velocity diagram along major axis of ^{13}CO emission. The cut is taken through the center of the ^{13}CO emission at a position angle of 18°. Contours in the channel maps are at 0.1 K (39 mJy beam^{-1}) intervals.

tion of the trailing spiral arm visible in the optical (Fig. 2a, gray scale). If the inflow were not uniform about the disk but restricted to the NE and SW regions along the extended molecular bar, the required inflow velocity could be higher since the bar is aligned within 5°–10° of the major axis of the galaxy and thus any radial velocities there would be nearly perpendicular to the line of sight. The determination of radial motion in the outer regions of the bar is much more ambiguous because of the close alignment of the bar with the major axis and the limited velocity information here (the bar is not sufficiently well resolved to show the inclination of the isovelocity contours that would indicate the presence of noncircular motions in the region). We see no evidence for the expanding "bubble" seen by Ishiguro et al. (1989) in the SW region of the bar. This may be because these noncircular motions occur in a region of lesser column density to the north of the bar that does not appear in our ^{13}CO maps.

The velocity dispersion of the gas is illustrated in Figure 3*c*, presenting the second velocity moment of the emission, $\Delta v = \{[\int (v - \bar{v})^2 T_b\, dv]/(\int T_b\, dv)\}^{1/2}$, which for a Gaussian gas distribution can be related to the full width half-maximum by $V_{FWHM} = \ln 4\, \Delta v$. The central $\sim 10''$ (240 pc) has a markedly higher velocity dispersion than the rest of the region, reaching a peak of $\Delta v \cong 70$ km s^{-1} or $V_{FWHM} \cong 160$ km s^{-1}. Inspection of line spectra in this region indicate that the full width at zero intensity is as large as $V_{FWZI} \cong 200$ km s^{-1}. This large dispersion probably reflects a steeply-rising rotation curve in the inner 120 pc that is spatially unresolved in our 150 pc beam. The dispersion falls off smoothly with distance from the nucleus from values of $V_{FWHM} \sim 120$–160 km s^{-1} in the nucleus to 70–90 km s^{-1} mid-bar to $V_{FWHM} \sim 25$–70 km s^{-1} in the outer regions. Outside the nucleus, the apparent drop-off in dispersion is spatially resolved and therefore likely a real effect. These line widths are all higher than typical line widths observed in the Galactic disk (Burton & Gordon 1978; Scoville et al. 1987), $V_{FWHM} \sim 9$–12 km s^{-1}, but comparable to those observed in Galactic center clouds (Bally et al. 1988).

3. MOLECULAR STRUCTURE OF THE STARBURST

3.1. *Molecular Distribution, Column Densities, and Mass*

The spatial coincidence of the molecular gas as traced by ^{13}CO and the 6 cm continuum emission of the starburst has important implications for the formation of the starburst. In Maffei 2, there is a coherent structure to the starburst: from the radio continuum map of Figure 3*a* it is apparent that the most vigorous star formation is proceeding along a linear feature ~ 300 pc in length, although there is radio continuum emission along the full 1 kpc extent of the bar. The crossing time of the region would be 5×10^7 yr for gas moving at a sound speed of 10 km s^{-1}, or an order of magnitude longer at typical molecular cloud sound speeds. This crossing time is comparable to the lifetime of the massive stars within the burst and probably the lifetime of the starburst as well. Given that this crossing time scale is long compared to the burst lifetime, how is relative simultaneity maintained across the starburst region and why does the starburst have a coherent structure? In some galaxies, enhanced star formation may be the result of some spatially selective triggering mechanism such as cloud collapse stimulated by compression from a nuclear jet (e.g., NGC 541; van Breugel et al. 1985). In Maffei 2, the correlation seen in Figure 3*a* between the molecular gas density and the 6 cm emission associated with the star formation strongly suggests that the structure of the starburst in Maffei 2 is regulated by the spatial distribution of the molecular gas, and not by a linear triggering mechanism.

The ^{13}CO emission has a single intensity peak coincident with the 6 cm continuum peak and is more closely correlated with the radio continuum than is the double-lobed ^{12}CO structure observed by Ishiguro et al. (1989). We expect that the ^{13}CO maps reflects the molecular density distribution more accurately than ^{12}CO because of lower optical depths in the ^{13}CO line. From the ^{12}CO channel maps of Ishiguro et al., we estimate that the $T_{^{12}CO}:T_{^{12}CO}$ ratio in the nuclear gas is typically 6–15 in Maffei 2, consistent with ^{12}CO optical depths of ~ 2–7 if we assume $[^{12}CO]/[^{13}CO] = 40$ and the excitation temperatures for the ^{12}CO and ^{13}CO gas are the same. The corresponding ^{13}CO optical depths are 0.05–0.2.

The difference in morphology between the ^{12}CO and ^{13}CO maps of Maffei 2 (or equivalently, the variation in the integrated intensity ratio $I_{^{12}CO}:I_{^{13}CO}$) is not easily understood. If ^{12}CO samples only the outer envelopes of optically thick clouds, any region-to-region variation in the average molecular cloud size could affect the integrated intensity ratios. If the average cloud size is smaller in the SW portion of the bar than in the NE, the corresponding increase of surface area to unit volume of molecular material would yield correspondingly higher fluxes in ^{12}CO than ^{13}CO. Another way of explaining the variation in the integrated intensity ratio is by a variation in excitation temperature. If T_{ex} is enhanced in the SW region, the optically thick ^{12}CO emission will be enhanced while the optically thin ^{13}CO emission will be suppressed, although this may be offset to some degree by temperature-dependent fractionation (Frerking, Langer, & Wilson 1982; van Dishoeck & Black 1988). It is also possible that temperature gradients within the clouds cause, for instance, ^{12}CO to trace the outer, warmer parts of the clouds while ^{13}CO traces the inner, cooler parts. Without additional information we cannot rule out any of these possibilities.

Since the ^{13}CO is optically thin, we can derive column densities, visual extinctions, and masses from the observed inte-

grated intensities. The observed dust temperature in the inner 50″ of Maffei 2 is $T_d \sim 47$ K (Rickard & Harvey 1983); if we assume the dust temperature reflects the kinetic temperature ($T_K = T_d$) and that the CO is thermalized ($T_{ex} = T_K$), we may reasonably adopt an excitation temperature $T_{ex} = 50$ K. For the observed range of integrated intensity $I_{CO} = 9$–90 K km s^{-1} we obtain $N_{^{13}CO} = 0.26$–2.6×10^{17} cm^{-2}. To convert to H_2 column densities we need the abundance ratio $[^{13}CO]/[H_2]$. Estimates of $[^{13}CO]/[H_2]$ range from 2.0×10^{-6} ($A_V \lesssim 2$ mag; Dickman 1978) to 1.0–1.4×10^{6} (Frerking, Langer, & Wilson 1982), with much of the uncertainty due to temperature-dependent CO fractionation effects (e.g., Frerking, Langer, & Wilson 1982; van Dishoeck & Black 1988). We adopt $[^{13}CO]/[H_2] = 2.0 \times 10^{-6}$, consistent with $[^{12}CO]/[^{13}CO] = 40$ and $[^{12}CO]/[H_2] = 8.5 \times 10^{-5}$ (Black & Willner 1984). The observed range of H_2 densities is then $N_{H_2} = 1.3$–13×10^{22} cm^{-2}. This range in column density corresponds to molecular mass surface densities of $\sigma_{H_2} =$ 200–2000 $M_\odot$ pc^{-2}—high compared to typical Galactic surface densities ($\sigma_{H_2} \sim 5$ $M_\odot$ pc^{-2} for the solar neighborhood; ~ 20 $M_\odot$ pc^{-2} for molecular regions; Sanders, Soloman, & Scoville 1984) but similar to those observed in the centers of our own (Sanders, Soloman, & Scoville 1984) and other spiral galaxies (Young 1987).

The visual extinctions implied by these column densities can be considerable. For $N_{H_2}/A_V = 0.94 \times 10^{21}$ (Bohlin, Savage, & Drake 1978; Cardelli, Clayton, & Mathis 1988), we calculate extinctions of $A_V \simeq 14$–140 mag. This is consistent with the high visual extinctions derived from mid-infrared observations of similar starburst galaxies (Lebofsky & Rieke 1979; Beck, Beckwith, & Gatley 1984; Roche & Aitken 1985) given the fact that near-infrared extinction estimates saturate at $A_V \gtrsim 20$ mag. Although gas-based estimates of extinction are indirect and sensitive to variations in the dust-to-gas ratio, the accumulating evidence from these independent methods indicate that extinctions of $A_V \gtrsim 15$–20 mag are common within starburst regions.

From the integrated ^{13}CO flux of $S_{^{13}CO} = 148$ Jy km s^{-1} we calculate a molecular hydrogen mass of $M_{H_2} = 2.3 \times 10^{8}$ $M_\odot$, which corresponds to the total gas mass (including He) of $M_{gas} = 3.1 \times 10^{8}$ $M_\odot$. This is an underestimate to the total mass since we have used a conservative value of $[^{13}CO]/[H_2]$ and we have lost $\sim 35\%$ of the ^{13}CO flux due to missing short spacings. Within the inherent uncertainties of the $[^{13}CO]/[H_2]$ abundance ratio, this H_2 mass is in good agreement with those derived independently from interferometer maps of optically thick ^{12}CO by Ishiguro et al. (1989; 2.4×10^{8} $M_\odot$) using the standard Galactic conversion factor $N_{H_2}/I_{^{12}CO}$ (Scoville & Sanders 1987). Apparently the Galactic $N_{H_2}/I_{^{12}CO}$ conversion factor is appropriate for the nuclear Maffei 2 clouds in spite of the fact that the overall gas temperature is likely to be significantly higher than in Galactic clouds.

We can estimate an overall star formation efficiency for the region from our derived molecular mass and the observed massive star formation rate. We define massive star formation efficiency here as the ratio of molecular gas mass to the mass of massive young stars, M_{OB}/M_{gas}. The mass in massive young stars, M_{OB}, can be determined from an estimate of the Lyman continuum rate under the assumption of an initial mass function (IMF). An estimate of the thermal radio continuum flux gives a total ionization rate of $N_{Lyc} = 7 \times 10^{52}$ s^{-1} for the entire ^{13}CO region (Turner & Ho 1991). This Lyman continuum rate corresponds to $L_{OB} \sim 6 \times 10^{9}$ $L_\odot$ for the Miller-Scalo IMF (Scalo 1986; Panagia 1973; Maeder & Meynet 1989) for stellar mass limits of 60 and 7 $M_\odot$ (spectral types O8.5 and B3), which is consistent with the observed far-infrared luminosity of $L_{FIR} = 4 \times 10^{9}$ $L_\odot$ (Rickard & Harvey 1984). For this IMF, the mass in massive young stars corresponding to this luminosity is $M_{OB} \sim 6 \times 10^{6}$ $M_\odot$. A lower limit to the star formation efficiency in the Maffei 2 starburst, M_{OB}/M_{gas}, is therefore $\sim 4\%$ over the 300 pc extent of the starburst region containing $\sim 50\%$ of the observed molecular gas. If the starburst IMF extends down to stars as small as 0.5 $M_\odot$, the total star formation efficiency increases to $\sim 20\%$. This efficiency is determined for our 150 pc beam and may be higher locally. The latter efficiencies are high compared to those observed in Galactic massive star-forming regions, where observed efficiencies are $\lesssim 5\%$ on 20–60 pc size scales (e.g., Duerr, Inhoff, & Lada 1982) although the efficiency may be higher on smaller size scales (e.g., Sargent 1979). If the IMF in the Maffei 2 starburst is restricted to high-mass stars, the efficiencies are closer to the Galactic values. The luminosity-to-mass ratio, an IMF–independent measure of the star formation efficiency, is $L_{FIR}/M_{H_2} = 20$ $L_\odot/M_\odot$ in Maffei 2. This is also indicative of an unusually efficient star formation rate in this region since it is significantly higher than Galactic clouds without H II regions ($\langle L/M \rangle \sim 1$ $L_\odot/M_\odot$) or Galactic clouds with H II regions ($\langle L/M \rangle \sim 7$ $L_\odot/M_\odot$) (Scoville & Good 1989), but similar to the values in other galaxies with moderate starbursts (Sanders et al. 1988).

If we assume an average lifetime for the massive stars in this mass range of 10^7 yr (Maeder 1983), the steady state massive star formation rate required to sustain the 6 cm continuum luminosity is ~ 0.3 $M_\odot$ yr^{-1}. This is comparable to the massive star formation rate in the entire Galaxy (Scalo 1986), but nearly an order of magnitude lower than that of M82 or NGC 253. The equivalent star formation rate per pc^2 computed over the nuclear starburst is SFR ~ 5000 $M_\odot$ Gyr^{-1} pc^{-2}. This star formation rate is on the order of 50 times larger than the peak rates in the spiral arms of M51 (Lord & Young 1990). Since the molecular surface density in Maffei 2 is also higher than the M51 arms, the peak star formation efficiency is higher in Maffei 2, but only by factors of 2–5. Some of this apparent increase in efficency may be due to our truncated IMF (60–7 $M_\odot$) compared to that employed by Lord and Young (100–0.1 $M_\odot$), although a preferentially high-mass IMF is likely to be appropriate for a starburst region (Rieke 1991). This comparison suggests that the enhanced star formation rate in the nucleus of Maffei 2 is primarily a result of the increased molecular gas density.

The star formation efficiency SFR/$\sigma_{H_2} \sim 2$ Gyr^{-1} suggests a time scale for gas depletion within the starburst of 5×10^{8} yr unless significant amounts of gas are returned to the region in molecular form on these time scales. This time scale could be shorter than 10^8 yr if low-mass stars are included. Although there may eventually be replenishment of the gas from mass-losing stars (e.g., Norman & Scoville 1978), the gas returned may not be in a form (molecular) to support star formation at the current rate. Given the disruptions suffered by the region in the form of stellar winds and SNR from the massive stars, the actual duration of the burst is likely to be shorter. Therefore we regard 10^8 yr as an upper limit to the lifetime of the Maffei 2 starburst.

3.2. *Nuclear Gas Dynamics and the Molecular Bar*

The dynamics of the nuclear molecular gas in Maffei 2 differ markedly from that of Galactic disk molecular gas, which has possibly contributed to the development of the starburst in Maffei 2. Although different from the dynamics of Galactic disk molecular gas, in many respects the kinematics and distribution of molecular gas in the nucleus of Maffei 2 may be similar to that of the Galactic Center although its azimuthal structure is difficult to evaluate unambiguously.

The position-velocity diagram of the ^{13}CO emission, comprised of a cut along the major axis of the bar, is presented in Figure 4. The observed velocities are symmetric about $\alpha = 2^h38^m8^s.25 \pm 0^s.15$, $\delta = 59°23'27 \pm 2''$, which we adopt as the dynamical center of Maffei 2. We obtain a velocity centroid of $V_{sys} = -10 \pm 5$ km s^{-1} from the ^{13}CO. This centroid is slightly different from that of the large-scale H I distribution, $V_{H\,I} \sim -20$ km s^{-1} (Bottinelli et al. 1971; Hurt, Turner, & Ho 1991). Although the asymmetries in the emission make it difficult to determine, there may be an offset in the centroids of the high- and low-velocity gas, with the high-velocity nuclear gas centered at ~ -5 km s^{-1}, and the low-velocity gas at -15 km s^{-1}, closer to the H I value. The rotational velocities in the center of the nuclear region rise steeply to a peak value of $V_{obs} = 100$ km s^{-1} at a radius of 120 pc from the nucleus, as can be seen in Figure 4. Corrected for inclination, this velocity corresponds to a circular velocity $V_{circ} = 110$ km s^{-1}. Correction for the orientation of the inner portion of the bar 10°–15° off the major axis of the galaxy further increases this estimate to $V_{circ} = 120$–130 km s^{-1}. The rotation curve then falls off to a value of 90 km s^{-1} and remains flat out to the limits of the ^{13}CO emission at a radius of ~ 500 pc.

The steeply rising rotation curve within the central 120 pc is indicative of rapidly rotating gas in a region of high uniform mass density, creating a "solid body" rotating region. The isovelocity contours in this region (Fig. 3*b*) are consistent with "solid body" rotation. The position-velocity diagram (Fig. 4) shows that the majority of gas in this inner region is clumped at the low- and high-velocity ends of the rotation curve and does not fill in the rising rotation curve. One interpretation of this result is that the molecular gas forms a ring around a compact ($r < 120$ pc) stellar cluster. This central peak rotation velocity of 120–130 km s^{-1} is high; it represents $\sim 70\%$ of the maximum H I rotation velocity attained at a radius of 6 kpc (Hurt, Turner, & Ho 1991). Since this region is less than two full beam widths in total extent, the turnover may actually occur at a radius smaller than 120 pc, although this figure is good to within a factor of 2. Steeply rising rotation curves followed by turnovers are seen in the nuclei of other spiral galaxies. In M31, the turnover at 1″ or 3–4 pc from the dynamical center may be indicative of a black hole (Kormendy 1988; Dressler & Richstone 1988). In the Galaxy, the rotation curve reaches a peak velocity of 120 km s^{-1} at a galactocentric radius of 40 pc (Lizt & Burton 1978; Bally et al. 1988), falling off in an intermediate Keplerian region extending from ~ 100–200 pc. Here, as in Maffei 2, the "pointlike" central gravitational potential could be created by a dense stellar cluster within the inner ~ 100 pc.

From our ^{13}CO rotation curve, we estimate the dynamical (or gravitational) mass within this inner Keplerian region to be $M_{dyn} = 4 \pm 1 \times 10^8\ M_\odot$ for the inner 5″ (120 pc), assuming a spherical mass distribution. Formally this is an upper limit to the true mass, which may be up to a factor 2 smaller if the mass distribution is flattened; however, from the rapidly rising rotation curve we might expect the mass in this region to be close to spherical. This is roughly the same mass as inferred for the inner 120 pc of our own Galactic center (Genzel & Townes 1987). This region contains 50% ± 10% of the ^{13}CO flux and a molecular mass of $M_{H_2} \sim 1.2 \times 10^8\ M_\odot$. Thus $\sim 30\%$ of the total mass in the center of Maffei 2 is molecular hydrogen (40% including helium). This is significantly higher than the 10%–15% molecular (H_2) mass fraction typical of the Galactic disk (Sanders, Solomon, & Scoville 1984). However, a high (20%) molecular mass fraction has also been suggested for the innermost 2.5 kpc of our own Galactic Center (Linke, Stark, & Frerking 1981).

The fact that the gas mass is a significant fraction ($\sim 40\%$) of the total mass in the nucleus suggests that gas as well as stars play an important role in the nuclear dynamics. Yet this molecular component is located 5″ (120 pc; corresponding to a gravitational energy of $\sim 10^{55}$ ergs) off the dynamical center of the galaxy. This implies that the nuclear dynamics are to some degree nonaxisymmetric. A similar situation may well hold in our own Galaxy, where the substantial molecular component appears to be located preferentially at positive longitudes.

Another unusual aspect of this molecular cloud complex is that the dynamical lifetime against differential rotation of the structure outside the solid body rotation region is very short. This may also be true of the nuclear bars seen in IC 342 (Lo et al. 1984; Ishizuki et al. 1990) and NGC 6946 (Ball et al. 1985). In Maffei 2, the rotational period of gas for circular rotation at the 5″ (120 pc) velocity peak is 5×10^6 yr. Differential rotation between this region and the outer bar at a radius of 10″ (240 pc) will cause "winding up" of the bar by $\pi/2$ in $\sim 2 \times 10^6$ yr. If this feature is indeed a bar, either it is a very transient ($\sim 10^6$ yr) phenomenon, or its structure must be maintained by some mechanism such as density waves. The fact that the massive stars and their SNR are so well correlated with the molecular bar suggests that the lifetime of this feature is at least as large as massive stellar lifetimes, $\sim 10^7$ yr. The presence of molecular bars in the nuclei of other nearby galaxies also suggests that nuclear bars are not extremely short-lived phenomena.

Molecular gas in the nucleus of Maffei 2 is characterized by three distinct features that distinguish it from molecular gas in typical galactic disks: (1) the gravitational potential is to a large extent governed by a spherical central star cluster; (2) $\sim 40\%$ of the total mass is in the form of molecular gas (including He), and this relatively massive component is offset by ~ 120 pc from the dynamical center of the galaxy; (3) the dynamical lifetime of non-axysymmetric structures in this region is extremely short, $< 2 \times 10^6$ yr. Given these circumstances, how did the molecular bar form and how does it exist? Why is this component offset from the dynamical center? Stellar bars are observed to be significantly (0.5–1 kpc) offset from the dynamical centers of very late type spirals, in particular, in Magellanic barred galaxies (Freeman 1975). However, Maffei 2 is not likely to be a late-type spiral, and the offset bar feature is gaseous and nonstellar.

A model that may be applicable here is the circumstellar disk model of Adams, Ruden, & Shu (1989), in which they find that massive ($\gtrsim 25\%$ of the total system) gaseous circumstellar disks are unstable to single arm spiral modes. Although the Adams, Ruden, and Shu model was developed to explain accretion disks about young stellar objects, many of the features of these systems (massive disks; Keplerian rotation curves) are similar to those found in the nucleus of Maffei 2. Such $m = 1$ modes have also been proposed to explain nonsymmetric star formation in the bars of Magellanic-type spirals (Odewahn 1991) We estimate that the Toomre stability factor $Q =$

$(\kappa \Delta v)/(\pi G \sigma_{gas}) = 0.2$–$0.6$ for gas in this region, where $\kappa = 2\Omega$ and Δv is the observed ^{13}CO line width. The fact that $Q \leq 1$ indicates that although the rotational velocity and line width (indicating the effective gas pressure) are large, the high molecular surface densities that we observe are sufficient to offset these stabilizing influences. The molecular gas in the nucleus of Maffei 2 may well be unstable to the growth of density waves. It is therefore possible that a stable mode in the gaseous disk might explain the longevity and off-axis nature of the molecular bar and starburst.

4. CONCLUSIONS

We find that the ^{13}CO gas in the nucleus of Maffei 2 is optically thin and is thus a good tracer for the overall molecular gas distribution. The gas lies in a slightly curving bar, 1 kpc in extent, reminiscent of spiral arms. The molecular gas density is highly correlated with the starburst regions as traced by 6 cm continuum emission. This suggests that the enhanced star formation, at a massive star formation efficiency M_{OB}/M_{gas} that is roughly constant at $\gtrsim 4\%$ across the region (and possibly as high as 20% for an IMF extending to 0.5 $M_\odot$ stars) is determined by the molecular gas density distribution in the nucleus and not by some other spatially selective triggering mechanism such as cloud collapse induced by a nuclear jet.

We calculate a total molecular mass of $M_{H_2} = 2.3 \times 10^8$ $M_\odot$, and a total gas mass, including He, of $M_{gas} = 3.1 \times 10^8$ $M_\odot$ in the ^{13}CO bar. The H_2 surface densities are high, $\sigma_{H_2} =$ 200–2000 $M_\odot$ pc^{-2}, as are the visual extinctions, $A_V \sim 14$–140 mag across 150 pc size scales. For a star formation rate of ≥ 0.6 $M_\odot$ yr^{-1} indicated by the infrared luminosity and radio continuum flux, the molecular gas in the nucleus of Maffei 2 will be consumed in $\lesssim 10^8$ yr in the absence of molecular replenishment. This, and the fact that the star formation rate is up to 50 times greater than peak star formation rates observed in spiral disks, indicate that the star formation in the nucleus of Maffei 2 is indeed a "burst."

The bar structure shows very steeply rising velocities, peaking at 120–130 km s^{-1} at a 120 pc radius. This central "solid body" region is followed by a near-Keperian fall-off to a flat rotation curve extending out to the limits of ^{13}CO emission at a radius of 500 pc. We see no evidence of strong noncircular motions in the ^{13}CO. The circular velocities in the inner 120 pc region correspond to a spherical dynamical mass of $\sim 4 \times 10^8$ $M_\odot$. Gas (including He) constitutes 40% of the total mass in the "solid body" region, and it is here that the strongest star formation activity occurs.

The high angular velocities and differential rotation within the nuclear region imply that the molecular bar has a dynamical lifetime against "winding up" of $\sim 2 \times 10^6$ yr. We speculate that the presence of bars in the nuclei of other spiral galaxies as well as the correlation of the molecular bar with the massive stars and SNRs of the starburst imply a longer lifetime for this bar feature, which would necessitate some mechanism for its longevity such as spiral density waves.

We would like to thank Anneila Sargent and Nick Scoville for comments on early versions of this paper. We are grateful to Hyron Spinrad for providing the optical photo of Maffei 2 and Derek Wills and Patrick McCarthy for the optical astrometry. We also thank Steve Padin, Steve Scott, and Dave Woody for their kind assistance during the observations. This research was supported in part by grant CS-57-88 from the California Space Institute. The Owens Valley Millimeter Interferometer is operated with support from Caltech and the NSF AST 87-14405 with additional operations support from UCLA.

REFERENCES

Adams, F. C., Ruden, S. P., & Shu, F. H. 1989, ApJ, 347, 959
Ball, R., Sargent, A. I., Scoville, N. Z., Lo, K. Y., & Scott, S. C. 1985, ApJ, 298, L21
Bally, J., Stark, A. A., Wilson, R. W., & Henkel, C. 1988, ApJ, 324, 223
Beck, S. C., Beckwith, S., & Gatley, I. 1984, ApJ, 279, 563
Becklin, E. E., Gatley, I., Matthews, K., Neugebauer, G., Sellgren, K., Werner, M. W., & Wynn-Williams, C. G. 1980, ApJ, 236, 441
Black, J., & Willner 1984, ApJ, 279, 673
Bohlin, R. C., Savage, B. D., & Drake, J. F. 1978, ApJ, 224, 134
Bottinelli, L., Chamaraux, P., Gerard, E., Gouguenheim, L., Heidmann, J., Kazes, I., & Lauque, R. 1971, A&A, 12, 264
Burton, W. B., & Gordon, M. A. 1978, A&A, 63, 7
Burton, W. B., & Liszt, H. S. 1978, ApJ, 225, 815
Buta, R. J., & McCall, M. L. 1983, MNRAS, 205, 131
Cardelli, J. A., Clayton, G. C., & Mathis, J. S. 1988, ApJ, 329, L33
Condon, J. J., Condon, M. A., Gisler, G., & Puschell, J. J. 1982, ApJ, 252, 102
Dickman, R. L. 1978, ApJS, 37, 407
Dressler, A., & Richstone, D. 1988, ApJ, 234, 701
Duerr, R., Inhoff, C. L., & Lada, C. J. 1982, ApJ, 261, 135
Ekers, R. D. 1975, in Structure and Evolution of Galaxies, ed. G. Setti (Dordrecht: Reidel), 217
Freeman, K. 1975, in Stars and Stellar Systems, Vol IX, ed. A., Sandage, M., Sandage, & J. Kristian (Chicago: University of Chicago), 409
Frerking, M. A., Langer, W. D., & Wilson, R. W. 1982, ApJ, 262, 590
Genzel, R., & Townes, C. H. 1987, ARAA, 25, 377
Ho, P. T. P., Beck, S. C., & Turner, J. L. 1990, ApJ, 349, 57
Ho, P. T. P., Turner, J. L., Fazio, G. G., & Willner, S. P. 1989, ApJ, 344, 135
Ho, P. T. P., Turner, J. L., & Martin, R. N. 1987, ApJ, 322, L67
Hurt, R. L., Turner, J. L., & Ho, P., 1991, in preparation
Ishiguro, M. et al. 1989, ApJ, 344, 763
Ishizuki, S., Kawabe, R., Ishiguro, M., Okumura, S. K., Morita, K.-I., Chikada, Y., & Kasuga, T. 1990, Nature, 344, 224
Israel, F. P. 1980, A&A, 90, 246
Kormendy, J. 1988, ApJ, 325, 128
Lebofsky, M. J., & Rieke, G. H. 1979, ApJ, 229, 111
Linke, R. A., Stark, A. A., & Frerking, M. A. 1981, ApJ, 243, 147
Liszt, H. S., & Burton, W. B. 1978, ApJ, 226, 790
Lo, K. Y., et al. 1984, ApJ, 282, L59
Lo, K. Y., Cheung, K. W., Masson, C. R., Phillips, T. G., Scott, S. L., & Woody, D. P. 1987, ApJ, 312, 547
Lord, S. D., & Young, J. S. 1990, ApJ, 356, 135
Maeder, A. 1983, A&A, 120, 113
Maeder, A., & Meynet, G. 1989, A&A, 210, 155
Morris, M., Polish, N., Zuckerman, B., & Kaifu, N. 1983, AJ, 88, 1228
Norman, C., & Scoville, N. Z. 1988, ApJ, 332, 124
Odewahn, S. C. 1991, AJ, 101, 829
Panagia, N. 1973, ApJ, 192, 221
Rickard, L. J., & Harvey, P. M. 1983, ApJ, 268, L7
———. 1984, AJ, 89, 1520
Rickard, L, Turner, B., & Palmer, P. 1977, ApJ, 218, L51
Rieke, G. H. 1991 in Massive Stars in Starbursts, ed. C. Leitherer, N. Walborn, T. Heckman, & C. Norman (Cambridge: Cambridge University Press)
Rieke, G. H., & Lebofsky, M. J. 1978, ApJ, 220, L38
Rieke, G. H., Lebofsky, M. J., Thompson, R. I., Low, F. J., & Tokunga, A. T. 1980, ApJ, 238, 24
Roche, P. F., & Aitken, D. K. 1985, MNRAS, 213, 789
Sanders, D. B., Soifer, B. T., Elias, J. H., Madore, B. F. Matthews, K., Neugebauer, G., & Scoville, N. Z. 1988, ApJ, 325, 74
Sanders, D. B., Solomon, P. M., & Scoville, N. Z. 1984, ApJ, 276, 182
Sargent, A. I. 1979, ApJ, 233, 163
Sargent, A. I., Sutton, E., Masson, R., Lo, K., & Phillips, T. 1985, ApJ, 289, 150
Scalo, J. M. 1986, Fund. Cosmic Phys., 11, 1
Scoville, N. Z., & Good, J. C. 1989, ApJ, 399, 149
Scoville, N. Z. & Sanders, D. B. 1987, in Interstellar Processes, ed. D. J. Hollenbach & H. A. Thronson, Jr. (Dordrecht: Kluwer), 21
Scoville, N. Z., Sun, M. S., Clemens, D. P., Sanders, D. B., & Waller, W. H. 1987, ApJS, 63, 821
Seaquist, E., Pfund, J., & Bignell, R. 1976, A&A, 48, 413
Shostak, G., Weliachew, L. 1971, ApJ, 169, L71
Spinrad, H. et al. 1971, ApJ, 163, L25
———. 1973, ApJ, 180, 351
Telesco, C. M., & Harper, D. A. 1980 ApJ, 235, 392
Tinsley, B. M. 1980, Fund. Cosmic Phys., 5, 287
Turner, J. L., & Ho, P. T. P. 1991, in preparation
van Breugel, W., Filippenko, A. V., Heckman, T., & Miley, G. 1985, ApJ, 293, 83
van Dishoeck, E. F., & Black, J. H. 1988, ApJ, 334, 771
Weliachew, L., Casoli, F., & Combes, F. 1988, A&A, 199, 29
Woody, D. P., Miller, R. E., & Wengler, M. J. 1985, IEEE Trans. Microwave Th. Tech., 33, 90
Young, J. S. 1978 in Star Formation in Galaxies, ed. C. J. Lonsdale Persson, (NASA CP 2466), 197